

# Nanoliter Segmented-Flow Sampling Mass Spectrometry with Online Compartmentalization

Michael Volný,<sup>†,‡</sup> Joelle Rolfs,<sup>†</sup> Bejan Hakimi,<sup>†</sup> Petr Fryčák,<sup>†,§</sup> Thomas Schneider,<sup>†</sup> Dingsheng Liu,<sup>†</sup> Gloria Yen,<sup>†</sup> Daniel T. Chiu,<sup>\*,†</sup> and František Tureček<sup>\*,†</sup>

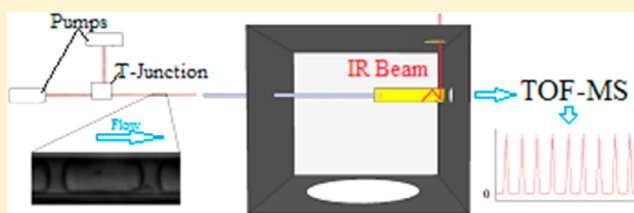
<sup>†</sup>Department of Chemistry, University of Washington, Seattle, Washington 98195, United States

<sup>‡</sup>Applied Physics Laboratory, University of Washington, Seattle, Washington 98105, United States

<sup>§</sup>Regional Centre of Advanced Technologies and Materials, Department of Analytical Chemistry, Faculty of Science, Palacký University, 17. Listopadu 12, 77146 Olomouc, Czech Republic

## S Supporting Information

**ABSTRACT:** We report a microfluidic device, using segmented flow in a two-phase system of immiscible liquids, which delivers aqueous droplets into a modified commercial mass spectrometer. The interface coupling the microfluidics to the mass spectrometer achieves up to 96% sample transfer efficiency to the vacuum chamber. Sample ionization is assisted by multipass infrared laser beam in the interface. The system achieves low femtomole detection limits of several analytes ranging from drugs to proteins. Sample ionization in this segmented-flow sampling was found to be remarkably insensitive to the presence of buffer salts and other matrices.



Introduction of solutions into mass spectrometers (MS) has become routine since the advent of electrospray ionization (ESI).<sup>1,2</sup> The homogeneous nature of solutions and the linear flow regime virtually guarantee a constant delivery of analytes dissolved in the solvent, which is essential for quantitative analysis. The concentration dependence of the electrospray ion signal<sup>3–5</sup> becomes a limiting factor when the sample is originally confined to a small volume, such as that of a single cell. For example, dissolving the content of a single cell, ranging from  $10^{-13}$  to  $10^{-12}$  L in volume, in a solvent volume of 1  $\mu$ L and subsequent introduction into the mass spectrometer by nanospray ionization results in a  $10^6$ -fold dilution of the cell components, e.g., from micromolar to picomolar. Such concentrations are not only at the limit of detection for methods using electrospraying, but also handling such highly diluted solutions is prone to contamination by other exogenous components obscuring or suppressing the analyte signal. These issues have been recognized for other concentration-dependent analytical methods, e.g., fluorescence spectroscopy and several approaches have been developed to overcome the dilution problem.<sup>6,7</sup> One approach relies on compartmentalization of the analyte solution into small volume droplets that are separated by an immiscible liquid in a channel of a microfluidic device.<sup>8–11</sup> Reducing the droplet volume reduces the dilution factor for the contents of a single cell and potentially results in concentrations that are more readily handled by ESI-MS or spectroscopic methods.<sup>12,13</sup> Droplet-based fluidics has been used in several approaches that used continuous<sup>14–16</sup> or discontinuous<sup>17–21</sup> sampling of single droplets into the mass spectrometer.

Here, we report a new system for coupling microfluidics to a simple mass spectrometer that achieves efficient sample delivery from compartmentalized aqueous droplets. Droplet microfluidics offer tools for manipulation of small volumes that are difficult to achieve by other means, while modern mass spectrometry provides superior detection capabilities. So far, the combination of both methods has been limited due to challenges in sample ionization because, under normal operating conditions, the immiscible biphasic composition of a liquid stream is poorly compatible with electrospray.<sup>17–21</sup> We report a new method that overcomes these limitations and achieves attomole limits of detection per a single compartment while demonstrating substantial robustness toward buffers, blood plasma, and other difficult matrices.

## EXPERIMENTAL SECTION

**Microfluidics.** Aqueous droplets (plugs) were generated by a microfluidic T-junction (IDEX Corporation) using fluorinated oil (perfluorohexane, Aldrich, Madison, WI) as the continuous phase (micrographs of the plugs can be found in the Supporting Information, Figure S1). The phase materials were injected into the channels using syringe pumps (KDS100, KD Scientific Holliston, MA). The mass spectrometer interface is compatible with any microfluidics channel or device that can be terminated by a capillary outlet. For the presented proof of principle experiments, the T-junction droplet generator was

Received: January 25, 2014

Accepted: March 13, 2014

Published: March 13, 2014

used as it allows nanoliter droplets to be produced at relatively low frequencies ( $\sim 10$  Hz). The capillaries used to build the microfluidics channel were standard coated fused silica 50/360  $\mu\text{m}$  (i.d./o.d.) (Polymicro Technologies, Phoenix, AZ). Perfluorohexane was selected as the immiscible phase of choice after a thorough study of different available liquids mainly because of its low boiling point and commercial availability.

**Mass Spectrometer.** A commercially available orthogonal reflectron time-of-flight mass spectrometer (Waters, Manchester, U.K.) was stripped of the standard Z-spray ion source and further modified to allow droplet sampling. In its original configuration, the LCT Premier consists of six differentially pumped regions, two of which were removed and replaced by the single manifold that allows transport of droplets into the vacuum and the subsequent evaporation and ionization of the droplets aqueous components. This manifold contains the interface described below.

**Interface.** A glass-lined stainless steel capillary (1.5 mm i.d., length 300 mm) was used to transfer the droplets from atmospheric pressure into the first vacuum region, evacuated by a roots blower (140 L/s; WAU 501, Leybold) to a pressure of  $\sim 1.5$  Torr. The glass-lined stainless steel inlet capillary was kept at a high potential (500 V) and aligned with the main axis of the ion optics. A gold plated tube lens (Epner Technologies, New York) was used inside the first vacuum region and also kept at a high potential of 400–500 V. The droplets were transported through this tube lens, which acts both as an electrostatic lens for freshly generated ions as well as a multireflection mirror for an IR-laser (25 W  $\text{CO}_2$  laser, Synrad, Bothell, WA, model 48-2,  $2\omega = 10.6 \mu\text{m}$ ,  $d = 3.5$  mm) used for droplet evaporation. The laser is guided into the first vacuum region through a ZnSe vacuum port and finally reflected by a mirror (both (Thorlabs, Newton, NJ) into the gold coated tube lens. The remaining power of the laser beam is dissipated into a block of anodized aluminum which was also mounted inside the vacuum manifold.

**Cells and Lysate.** Human breast cancer cells (MCF-7) were cultured in EMEM (Eagles Minimum Essential Media) growth media (American Type Culture Collection) with 10% fetal bovine serum (FBS) and 1% penicillin/streptomycin. The cells were rinsed 3 times via centrifugation and resuspension in DI water. The solution was then diluted to obtain a final concentration of  $1.2 \times 10^6$  cells/mL.

**Software.** The instrument control and data collection was performed using MassLynx 4.0 software (Waters). The spectra were then exported to Mmass 5.4 ([www.mmass.org](http://www.mmass.org)) for further processing. The Lipid maps database search at Lipidomics gateway (National Institute of General Medical Sciences) was performed using the embedded Mmass function.

## RESULTS AND DISCUSSION

**General Mode of Operation.** The new interface (Figure 1A) has a large inlet opening (1.5 mm) for efficient droplet introduction into the vacuum system and an ion transfer device, combining an electrostatic tube lens element with an infrared mirror. This combination allows for IR laser-assisted droplet evaporation in the rough vacuum region of the mass spectrometer and formation of gas-phase ions. Continuous streams of separated immiscible liquid phase compartments (water and fluorinated oil, Figure S1 in the Supporting Information) are generated in a microfluidic device which was realized as a polydimethylsiloxane (PDMS) chip,<sup>22</sup> or a fused silica capillary T-junction. The stream is converted to

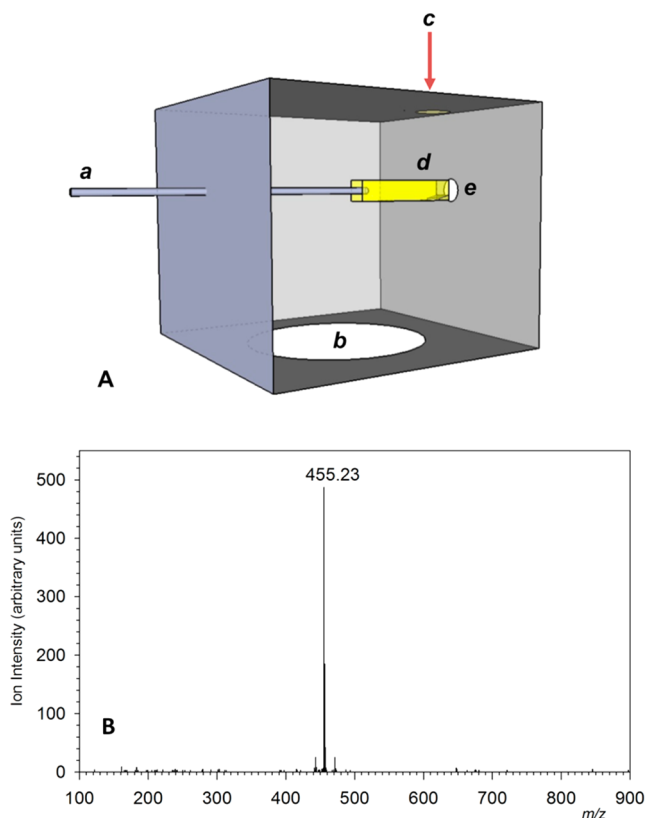


**Figure 1.** (Panel A) Schema of the interface for coupling of droplet microfluidics with mass spectrometry: a, capillary inlet (glass lined capillary); b, ISO-K 63 vacuum port; c, ZnSe IR transparent laser port; d, gold lined rectangular tube lens (see Figure S2 in the Supporting Information for details); e, aperture to the next vacuum region. (Panel B) Mass spectrum of 38 fmol of verapamil delivered in a single water compartment separated by immiscible plugs of perfluorohexane.

droplets and flown into the vacuum system. The droplets are evaporated by multipass laser beam in an IR-reflective electrostatic tube (Figure S2 in the Supporting Information), the content of the aqueous compartments is ionized, and the ions are transferred to the high-vacuum region and mass analyzed in a reflectron time-of-flight mass spectrometer. The oil phase is vaporized and pumped out before reaching the mass spectrometer. The mode of operation is quite simple. Charged droplets<sup>23</sup> are generated by applying a medium-high voltage (2–3 kV) at the tip of a fused silica capillary mounted at the exit from the microfluidic device. The aqueous or methanol droplets created from the tip are transported through the inlet capillary (1.5 mm i.d.) with up to 96% efficiency. This was rigorously determined for aqueous solutions of crystal violet in the following fashion. Droplets emitted from the tip and transmitted through the inlet capillary were collected in a small cup container inserted at the vacuum end of the capillary and the collected content was reanalyzed by a UV–vis assay to quantify sample recovery. This is analogous to the quantitative analysis used in soft landing of electrosprayed material.<sup>24</sup>

**Droplet Formation and Delivery.** Individual aqueous droplets were ionized and monitored by mass spectrometry in a continuous flow of a two-phase plug stream. For system testing purposes, the aqueous plugs were loaded with  $10^{-5}$  M verapamil that was monitored at  $m/z 455 \pm 1$ . The ion signal generated from aqueous plugs showed substantial stability over 30–120 s. The plug-to plug ion current variations were  $<20\%$

when plotted as the verapamil ion intensity at  $m/z$  455 (Figure S3 in the Supporting Information). At the typical flow rates, 45  $\mu\text{L}/\text{h}$  (12.5 nL/s) and 150  $\mu\text{L}/\text{h}$  (41.7 nL/s) for the water-based phase and perfluorohexane, respectively, the ion signal from a droplet showed a mean baseline width of 0.3–0.4 s and the peaks of adjacent droplets were spaced by approximately 0.5 s. Note that the ion signal drops to background level between two aqueous droplets, indicating that perfluorohexane does not efficiently ionize under these experimental conditions and generates negligible background signal in the mass spectrometer. Moreover, the perfect separation of ion signal from individual droplets illustrates that there was no mixing of content from adjacent aqueous plugs due to carryover in the microfluidics system.

Given the aqueous plug volume (3.8 nL) and verapamil  $10^{-5}$  M concentration, each plug contained 38 fmol of verapamil. The scan time of the mass spectrometer was set to 50 ms with 10 ms interscan delay, so that one plug of the verapamil solution roughly was sampled in five scans or 300 ms of data acquisition. The full mass spectrum in the  $m/z$  100–1000 range obtained by averaging a single plug over 300 ms is shown in Figure 1B. This shows the most abundant ion at  $m/z$  455, which corresponds to protonated verapamil, and very little background peaks in the mass spectrum. The spectrum in Figure 1B showed verapamil intensity of  $\sim 480$  counts. By averaging mass spectra of 10 randomly selected plugs of verapamil–water solution from the same experiment, we calculated the average intensity value per plug to be  $435 \pm 45$  counts, indicating a 10% plug-to-plug variation. The plug-to-plug repeatability mainly depended on the plug generation in the microfluidic T-junction and transport into the mass spectrometer at the tip of the fused silica capillary. Considering the background signal in the spectrum (2 counts), the above-calculated average verapamil signal for the 38 fmol plug was 73 times above the triple background level. This indicates that high attomole limits of detection for the verapamil load in a single plug are possible to achieve with this device. The estimated detection limits of the segmented-flow droplet method are higher than those reported previously for extractive electrospray and tandem mass spectrometric detection of highly ionizable analytes in an ion trap.<sup>25</sup> This is possibly due to the larger droplet size produced by our method and a lower charge-to-mass ratio. However, this is compensated by very low matrix effects in the segmented-flow droplet method, as discussed below.

**Large Molecular Mass Analytes.** The new sampling interface was found to work equally well for biopolymers. Figure 2A shows the spectrum of a single plug that contained 80 fmol of cytochrome c in water containing 0.5% of formic acid. The inset in Figure 2A shows the spectrum from a single plug flipped against the sum of spectra from several plugs illustrating the reproducibility of the protein charge states formed by droplet ionization. The most abundant peak corresponds to  $[\text{M} + 10\text{H}^+]^{10+}$  at  $m/z$  1236. The characteristic multiple charging of the protein analyte indicates that the ionization mechanism is not fundamentally different from the standard electrospray mechanism. Note that the spectrum shows no peak of dissociated heme at  $m/z$  616, indicating that protein transition from the droplet into the gas phase, as well as the ionization process forming the multiply charged states, were soft enough to prevent heme dissociation from the protein ion. Figure 2B shows the spectrum of a single plug containing 600 fmol of the cyclic peptide gramicidin-S in water ( $[\text{MH}]^+$  at  $m/z$

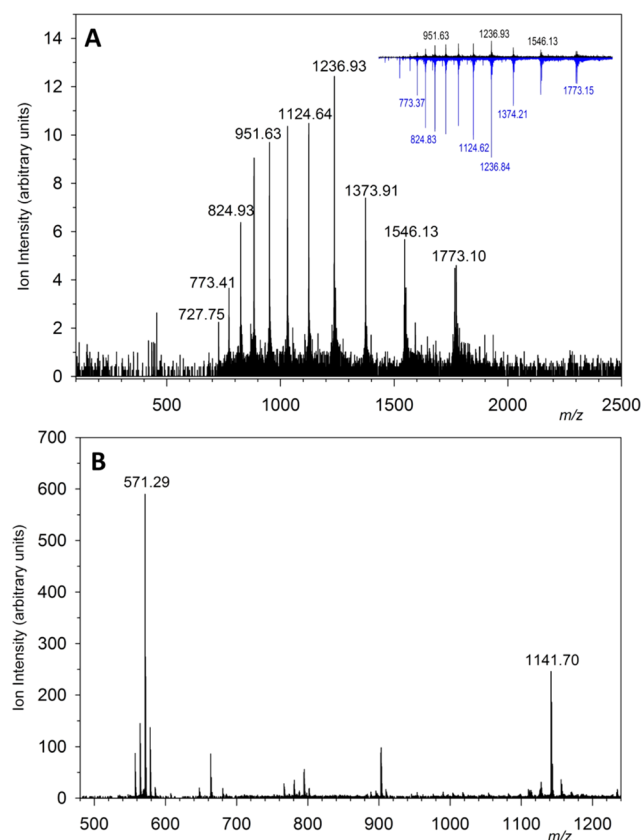


**Figure 2.** (Panel A) Mass spectrum obtained by recording the signal of a single plug containing 80 fmol of cytochrome c in water. The inset shows a sum of spectra obtained from several plugs, confirming the  $m/z$  assignment for individual charge states, flipped against the single plug spectrum. (Panel B) Mass spectrum obtained by recording the signal of a single plug containing 600 fmol of Gramicidin-S in water.

$m/z$  1141). The spectrum is dominated by a doubly charged ion at  $m/z$  571, pointing again to an electrospray-like ionization.

**Matrix Effects.** The potential for quantitative analysis of the droplet-MS system often depends on its sensitivity to the presence of various matrices. This was first tested by detecting verapamil in a mixture of three analytes (propranolol, verapamil, and reserpine) that were contained at  $10^{-5}$  M each in water plugs separated by perfluorohexane. The spectrum of the mixture showed practically no verapamil signal suppression due to the presence of the other analytes (Figure 3A).

In a still more stringent test, plugs of analytes were generated from concentrated PBS buffer containing 11.9 mM phosphate, 137 mM sodium chloride, and 2.7 mM potassium chloride. The mass spectrum in Figure 3B shows that propranolol and verapamil ions were formed albeit with  $\sim 4$ -fold signal suppression compared to a salt-free solution. The reserpine signal was almost completely suppressed. Under these high salt loading conditions, verapamil was the only analyte that also formed a significant sodium ion adduct at  $m/z$  477 (Figure 3B). Remarkably, even in the presence of the concentrated PBS buffer, the spectrum showed very low chemical noise due to the salt ions. This indicates that charged salt clusters were either not formed during droplet evaporation and subsequent ionization or were not transmitted from the interface into the instrument. By comparison, when the same solutions of these three analytes in water and PBS were electrosprayed on a Bruker LC Esquire ion trap and a Waters Quattro Micro



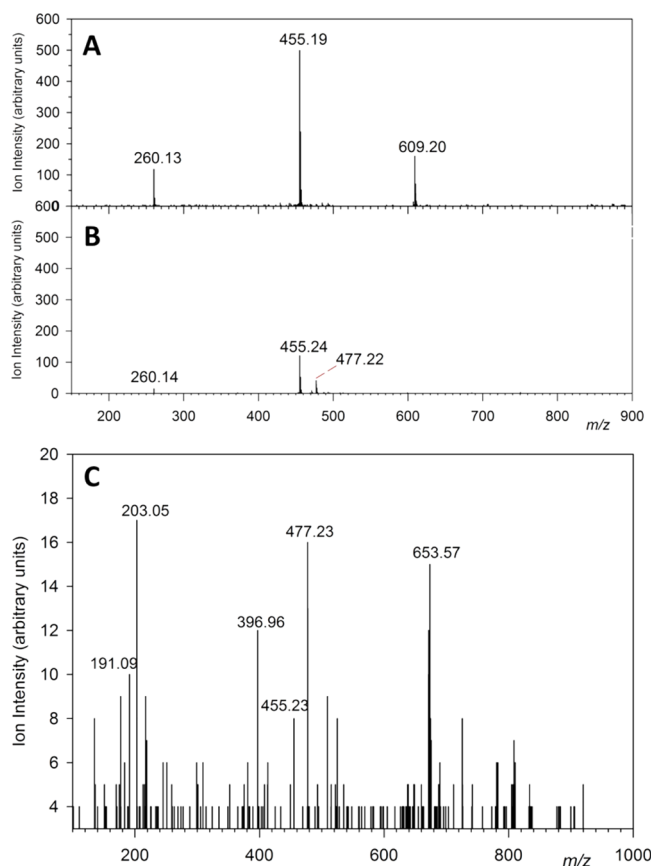


**Figure 3.** (Panel A) Mass spectrum obtained by recording signal of a single plug containing propranolol ( $m/z$  260), verapamil ( $m/z$  455), and reserpine ( $m/z$  609) in water. (Panel B) Mass spectrum obtained by recording signal of a single plug containing propranolol ( $m/z$  260), verapamil ( $m/z$  455), and reserpine ( $m/z$  609; suppressed) in PBS. The inset shows spectrum detail zoomed on verapamil proton and sodium adducts. Compared with the spectra in Figures S3 and S4 in the Supporting Information that show much poorer tolerance of PBS on commercial instruments. (Panel C) Mass spectrum obtained by recording signal of a single plug containing 20 fmol of verapamil ( $MH^+$   $m/z$  455;  $MNa^+$   $m/z$  477) in porcine blood plasma. Figure S7 in the Supporting Information shows comparison with the spectra obtained by summing of several plugs.

tandem quadrupole mass spectrometer, the spectra were strongly affected by PBS, and the reserpine peak at  $m/z$  609 was at the noise level. In addition, the spectra obtained on both instruments, the Bruker LC Esquire in particular, showed very high levels of chemical noise due to the PBS buffer (Figure S4 and S5, Supporting Information). Note that both these commercial instruments use heated gas at 200–250 °C to assist electrospray nebulization and droplet evaporation. The segmented-flow droplet method is clearly superior to standard heated-source electrospray in generating cleaner mass spectra.

Since the new droplet microfluidics interface demonstrated such a robust behavior toward high salt content, we attempted to analyze (i) porcine blood plasma mixed with verapamil solution in a 1:1 ratio to achieve a final concentration of verapamil in plasma at  $5 \times 10^{-6}$  M and (ii) a cell lysate spiked with verapamil and propranolol. In the first experiment, EDTA was added to the plasma and centrifuged at 10 000 rpm immediately before mixing with the verapamil solution. We were able to obtain mass spectra from plugs of plasma separated by perfluorohexane. Figure 3C shows a spectrum of a

single plasma plug that contained 20 fmol of verapamil. Interestingly, this spectrum is dominated by a sodium adduct ( $m/z$  477) whereas, in the PBS buffer, verapamil was predominantly protonated. The system was robust enough to perform several measurements, although it did suffer from occasional capillary clogging. Also, contamination of both the fluidics channels and inlet capillary was a problem in long-running experiments with untreated plasma.

In the other experiment, mammalian cell lysate (see the Supporting Information for the procedure) was spiked with verapamil and propranolol solutions to the final concentration of  $10^{-5}$  M. The original density of harvested cell suspension was  $10^6$  cells per mL, but after lysis the cell content was diluted so a single 5 nL plug containing  $\sim 1$ –10 cells. Plugs of this spiked cell lysate were successfully generated in a two phase flow system with perfluorohexane (Figure S6, Supporting Information), although the separation and plug-to-plug repeatability were worse than in the case of pure water or buffer solutions. The mass spectrum of a single plug of spiked cell lysate is shown in Figure 4A. It shows the peaks of protonated, sodiated, and potassiated propranolol with  $MH^+$ ,  $MNa^+$ , and  $MK^+$  at  $m/z$  260, 282, and 299, respectively, and verapamil with  $MH^+$ ,  $MNa^+$ , and  $MK^+$  at  $m/z$  455, 477, and 493, respectively (for a detailed zoom, see Figure 4B). The spectrum also showed peaks representing the content of approximately 10 lysed cells in two distinct mass regions. The

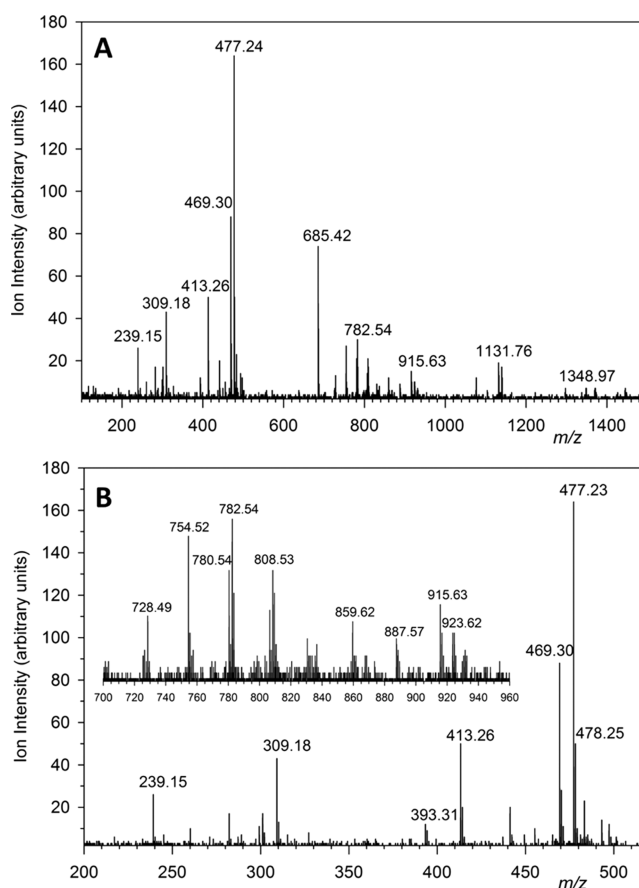


**Figure 4.** Mass spectrum obtained by recording signal of a single plug of lysed cells in water spiked with propranolol and verapamil. Panel A shows the overall spectrum. Panel B shows a spectrum zoomed on the lower  $m/z$  region of the spectrum in the main figure, while the inset shows a zoom on the glycerophospholipid region of the spectrum.

first region consisted of several peaks between  $m/z$  650 and 950 (inset in Figure 4B) that can be attributed to known glycerophosphopeptides. The lower mass region of  $m/z$  200–500 showed peaks that matched  $m/z$  of several fatty acids (Figure 4B). The assignments were made from a search in the Lipidmaps database at the Lipidomics gateway. The results of the search are given in (Figure S8 and Tables S1 and S2 in the Supporting Information). It should be noted that the search was performed with a 20 ppm mass accuracy limit and the results that are based only on  $m/z$  data must be viewed as a proof-of-the-principle concept, rather than a definite identification.

The above-described device for segmented flow introduces a dramatically simple delivery system for the generation of compartmentalized aqueous droplets. The system can be realized as a PDMS chip<sup>22</sup> or assembled from commercially available fused silica capillaries. A substantial improvement is the use of a volatile water-immiscible phase that avoids the need for removal of the oil phase from the microfluidics channel prior the ionization.<sup>17–19</sup> The capillary microfluidic system offers some advantages that facilitated the development of the interface, e.g., the fact that the individual parts were readily replaceable. A substantial advantage against microfluidics chips is the much more tolerant surface properties of fused silica compared to poly(dimethylsiloxane) (PDMS). This allowed us to experiment with a wide range of water-immiscible phases while avoiding surfactants to modify the surface tension in the aqueous droplets. The flow rates achieved with the capillary-based system (12 nL/s) were quite comparable to those used in microfluidic channels on standard chips.

A very important feature of the new microfluidic-MS system is its robustness toward high salt content in buffers and blood plasma. This is presumably related to rapid droplet evaporation in the IR laser beam that makes analyte ion desorption into the gas phase less sensitive to surface effects compared to ionization by electrospray. Another point worth emphasizing is that the interface can handle a continuous stream of plugs of water and perfluorinated oil at very low flow rates; such a solvent system is not efficiently ionized by standard electrospray. The TOF mass analyzer covers the entire mass range, e.g.,  $m/z$  100–1000 shown here, and not only a few channels as in the selected or multiple reaction monitoring modes used on tandem quadrupole instruments for ultrasensitive detection. Thus, our method allows multiple analytes, including unknowns, to be detected in the mass spectrum, not just those in a priori known and preselected channels. Further improvements in sensitivity and detection limits can undoubtedly be implemented by mating the interface with a mass spectrometer equipped with a more advanced ion optics, mass analyzer, and multichannel plate ion detector. The new method complements other approaches to ultrasensitive detection of single-cell content.<sup>26–30</sup>

## CONCLUSIONS

Segmented-flow microfluidics in combination with a new laser-assisted ionization interface provides a convenient means of delivering analyte cargo from aqueous droplets. The immiscible perfluorohexane liquid phase does not generate background ions in the positive ionization mode that would interfere with analyte ionization. The droplet method is remarkably robust toward the presence of buffers, salts, and other high-level matrix components. On the other hand, the formation of large (>10  $\mu\text{m}$ ) droplets decreases the ionization efficiency compared to electrospray, which somewhat compensates the high yield of

material delivery from the microfluidic device to the vacuum system of the mass spectrometer. Further efforts on improving the ion efficiency to achieve routine single cell analysis are in progress in this laboratory.

## ASSOCIATED CONTENT

### Supporting Information

Additional information as noted in text. This material is available free of charge via the Internet at <http://pubs.acs.org>.

## AUTHOR INFORMATION

### Corresponding Authors

\*E-mail: [chiu@chem.washington.edu](mailto:chiu@chem.washington.edu).

\*E-mail: [turecek@chem.washington.edu](mailto:turecek@chem.washington.edu).

### Notes

The authors declare no competing financial interest.

## ACKNOWLEDGMENTS

Financial support for this research was provided by the EUREKA Grant R01GM094905 from the NIH-NIGMS. P.F. gratefully acknowledges the support by the Operational Program Research and Development for Innovations-European Regional Development Fund and by the Operational Program Education for Competitiveness-European Social Fund (Projects CZ.1.05/2.1.00/03.0058 and CZ.1.07/2.3.00/20.0058 of the Ministry of Education, Youth and Sports of the Czech Republic).

## REFERENCES

- (1) Yamashita, M.; Fenn, J. B. *J. Phys. Chem.* **1984**, *88*, 4451–4459.
- (2) Yamashita, M.; Fenn, J. B. *J. Phys. Chem.* **1984**, *88*, 4671–4675.
- (3) Fernandez de la Mora, J.; Locortales, I. G. *J. Fluid Mech.* **1994**, *243*, 561–574.
- (4) Kebarle, P.; Ho, Y. In *Electrospray Ionization Mass Spectrometry, Fundamentals, Instrumentation and Applications*; Cole, R. B., Ed.; Wiley: New York, 1997; Chapter 1, pp 3–63.
- (5) Tang, L.; Kebarle, P. *Anal. Chem.* **1993**, *65*, 3654–3668.
- (6) Dada, O. O.; Huge, B. J.; Dovichi, N. J. *Analyst* **2012**, *137*, 3099–3101.
- (7) Amantonico, A.; Urban, P. L.; Fagerer, S. R.; Balabin, R. M.; Zenobi, R. *Anal. Chem.* **2010**, *82*, 7394–7400.
- (8) Song, H.; Tice, J. D.; Ismagilov, R. F. *Angew. Chem., Int. Ed.* **2003**, *42*, 768–772.
- (9) Song, H.; Chen, D. L.; Ismagilov, R. F. *Angew. Chem., Int. Ed.* **2006**, *45*, 7336–7340.
- (10) Song, H.; Li, H.-W.; Munson, M. S.; Van Ha, T. G.; Ismagilov, R. G. *Anal. Chem.* **2006**, *78*, 4839.
- (11) Chiu, D. T.; Lorenz, R. M.; Jeffries, G. D. M. *Anal. Chem.* **2009**, *81*, 5111–5118.
- (12) Pei, J.; Li, Q.; Kennedy, R. T. *J. Am. Soc. Mass Spectrom.* **2010**, *21*, 1107–1113.
- (13) Nie, J.; Kennedy, R. T. *Anal. Chem.* **2010**, *82*, 7852–7856.
- (14) Pei, J.; Qiang, L.; Lee, M.; Valaskovich, G. A.; Kennedy, R. T. *Anal. Chem.* **2009**, *81*, 6558–6561.
- (15) Li, Q.; Pei, J.; Song, P.; Kennedy, R. T. *Anal. Chem.* **2010**, *82*, 5260–5267.
- (16) Sun, S.; Slaney, T. R.; Kennedy, R. T. *Anal. Chem.* **2012**, *84*, 5794–5800.
- (17) Kelly, R. T.; Tang, K.; Irimia, D.; Toner, M.; Smith, R. D. *Anal. Chem.* **2008**, *80*, 3824–3831.
- (18) Fidalgo, L. M.; Whyte, G.; Ruotolo, B. T.; Benesch, J. L. P.; Stengel, F.; Abell, C.; Robinson, C. V.; Huck, W. T. S. *Angew. Chem., Int. Ed. Engl.* **2009**, *48*, 3665–3668.
- (19) Kelly, R. T.; Page, J. S.; Marginean, I.; Tang, K.; Smith, R. D. *Angew. Chem., Int. Ed.* **2009**, *48*, 6832–6835.
- (20) Zhu, Y.; Fang, Q. *Anal. Chem.* **2010**, *82*, 8361–8366.

- (21) Smith, C. A.; Li, X.; Mize, T. H.; Sharpe, T. D.; Graziani, E. I.; Abell, C.; Huck, W. T. *Anal. Chem.* **2013**, *85*, 3812–3816.
- (22) Liu, D.; Hakimi, B.; Volny, M.; Rolfs, J.; Chen, X.; Turecek, F.; Chiu, D. T. *Anal. Chem.* **2013**, *85*, 6190–6194.
- (23) He, W.; Baird, M. H. I.; Chang, J. S. *Can. J. Chem. Eng.* **1991**, *69*, 1174–1183.
- (24) Volný, M.; Tureček, F. *J. Mass Spectrom.* **2006**, *41*, 124–126.
- (25) Chen, H.; Venter, A.; Cooks, R. G. *Chem. Commun.* **2006**, 2042–2044.
- (26) Hiraoka, K.; Fukasawa, H.; Matshusita, F.; Aizawa, K. *Rapid Commun. Mass Spectrom.* **1995**, *9*, 1349–1355.
- (27) Baykut, G. *Introduction of ions from ion sources into mass spectrometers*. U.S. Patent 5,825,026, October 20, 1998.
- (28) Urban, P. L.; Jefimovs, K.; Amantico, A.; Fagerer, S. R.; Schmid, T.; Madler, S.; Puigmarti-Luis, J.; Goedecke, N.; Zenobi, R. *Lab Chip* **2010**, *10*, 3206–3209.
- (29) Issadore, D.; Humphry, K. J.; Brown, K. A.; Sandberg, L.; Weitz, D. A.; Westervelt, R. M. *Lab Chip* **2009**, *9*, 1701–1706.
- (30) Courtois, F.; Olguin, L. F.; Whyte, G.; Bratton, D.; Huck, W. T. S.; Abell, C.; Hollfelder, F. *ChemBioChem* **2008**, *9*, 439.